SEMARAK ILMU PUBLISHING

Journal of Advanced Research in Applied Mechanics

Journal homepage:
https://semarakilmu.com.my/journals/index.php/appl_mech/index
ISSN: 2289-7895

Numerical Simulation of RC Beams Strengthened with Near-Surface Mounted Fe-SMA Rebar

Muhammad Arif Ikmal Abdul Halim[1], Fariz Aswan Ahmad Zakwan[2], Lyn Dee Goh[1,*], Ruqayyah Ismail[2], Nor Hayati Abd Ghafar[3]

[1] Civil Engineering Studies, College of Engineering, Universiti Teknologi MARA, Cawangan Pulau Pinang, 13500 Permatang Pauh, Pulau Pinang, Malaysia
[2] Civil Engineering Studies, College of Engineering, Universiti Teknologi MARA, 40450 Shah Alam, Selangor, Malaysia
[3] Faculty of Civil Engineering and Built Environment, Universiti Tun Hussein Onn Malaysia, Batu Pahat, Johor, Malaysia

ARTICLE INFO

Article history:
Received 7 April 2023
Received in revised form 13 June 2023
Accepted 20 June 2023
Available online 4 July 2023

Keywords:
Iron-based shape memory alloy (Fe-SMA); prestressing forces; reinforced concrete (RC) beams; retrofitted structures

ABSTRACT

The utilisation of iron-based Shape Memory Alloy (Fe-SMA) to enhance the structural integrity of existing buildings and infrastructure has gained momentum in recent years. Prestressing forces induced by the shape memory effect of this smart material could be used to improve the behaviour of the structures. However, knowledge about this strengthening method is still limited, and more research is needed. This study explores the capability of reinforced concrete (RC) beams strengthened with Fe-SMA rebar through a numerical approach utilising ABAQUS. Past literature results were employed to verify the proposed finite element (FE) model in this study. The validated FE model was then used to identify the effects of Fe-SMA prestressing on the flexure performance of the RC beam. It is noted that the Fe-SMA strengthening improved the load-carrying capacities in the range of 14% and 47% of the RC beam. The application of Fe-SMA rebars can reduce the retrofitting cost effectively and improve the RC beam's flexural strength.

1. Introduction

A shape memory alloy (SMA), also known as a smart material, is a type of alloy that can be deformed when cold but returns to its predefined shape when heated. The recovery of the predefined shape is caused by its pseudoelastic properties and shape memory effect. In 1951, Chang and Read [1] developed SMAs based on the discovery of an Au-Cd alloy that contains the shape memory effect (SME). To date, numerous SMA types, such as NiTi-SMAs, Cu-Zn-AL SMAs, Cu-Al-Ni, and FeMnSi SMAs, have been discussed by Janke *et al.,* [2]. There are numerous applications of SMA in the industry [3]. In the aircraft industry, SMAs are being explored as vibration dampers for launch vehicles and commercial jet engines due to the large amount of hysteresis observed during pseudoelastic, allowing SMAs to dissipate energy and dampen vibrations. There is also strong interest in using SMAs for various actuator applications in the automotive and aircraft industries.

* *Corresponding author.*
E-mail address: gohlyndee147@uitm.edu.my

https://doi.org/10.37934/aram.108.1.1626

The demand for upgrading existing structures in the field of civil engineering has significantly risen over the past few decades as reported by Pirah *et al.,* [4]. Many researchers have conducted various studies on using SMAs as a construction material, and their findings have contributed valuable insights into the subject [5-10]. For example, an improvement in the structure's seismic performance can be achieved by damping the vibration applied to it using SMA with pseudoelastic behaviour [11,12]. There is also an interest in using SMA to strengthen the reinforced concrete (RC) structure. Initially, Soroushian *et al.,* [13] demonstrated the potential of Fe-SMA in improving the shear strength of the RC beam. Since then, many studies [2,14-18] have reported the promising results of strengthened RC beams using different techniques such as near-surface mounted (NSM) and external bonding and using SMA as internal reinforcements

The NSM technique is one of the most popular strengthening techniques. It is done by installing the strips or bars into the pre-cut grooves in the designated concrete area and then bonding them to the surrounding concrete with an epoxy adhesive or cementitious grout. For example, in a flexural member, the strengthening technique using NSM is executed at the tensile surface. This is evidenced in the studies conducted by [15,19,20], whereby the recovery stress in the SMA enhanced the serviceability of the RC members.

This study demonstrates the 3D finite element (FE) modelling of strengthened RC beams using ABAQUS software. The RC beam is assumed to be strengthened using Fe-SMA rebar, and this simulation could be done in a real-world application using the NSM technique. In real-world applications, a prestressing force is induced by the recovery stress generated by the Fe-SMA bar by heating it to the required temperature. This study applies monotonic static loads in a four-point configuration to the RC beam under study. The novelty of this study lies in its combination of investigating a new material (Fe-SMA rebar), using a 3D FE modelling approach, and exploring it as an NSM for RC beams. The findings of this study could potentially contribute to the development of more effective and efficient methods for strengthening RC beams.

2. Prestressing using Shape Memory Alloy

SMA has two main crystallographic phases. The low symmetry phase, called the martensite phase, exists at low temperatures, and the high symmetry phase, called the austenite phase, exists at high temperatures. According to Zhang *et al.,* [21], there are three microstructures of crystal lattices in SMA, i.e., γ-austenite (face-centred cubic structure, f_{cc}), ε-martensite (hexagonal close-packed structure, h_{cp}), and α-martensite (body-centred tetragonal structure, b_{ct}), as shown in Figure 1.

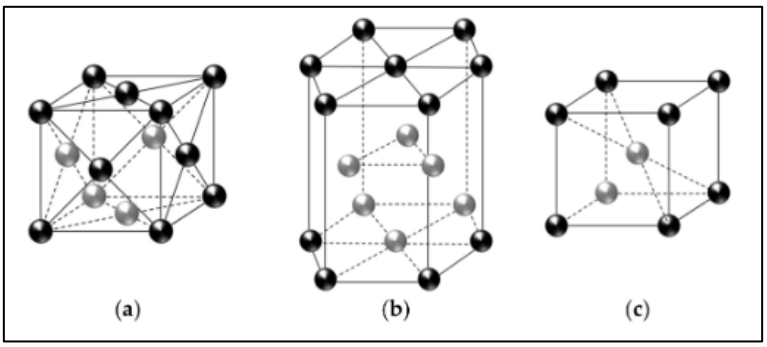

Fig. 1. Micro-structure of crystal lattices (a) γ -austenite (f_{cc}); (b) ε -martensite (h_{cp}), (c) α -martensite (b_{ct}) [21]

The alteration of the metal structure from γ-austenite to ε-martensite (phase transformation) happens when the material is subjected to either changes in temperature or external forces. The transformation of austenite to martensite is referred to as forward transformation. It happens when the material in the austenite phase cools down to a temperature below M_s (martensite start) and is fully transformed to martensite at M_f (martensite finish) temperature. The backward transformation takes place when the SMA at the martensite phase is heated above A_s (austenite start) and fully transformed to austenite at temperature A_f (austenite finish) [14]. The transformation phase is illustrated in Figure 2.

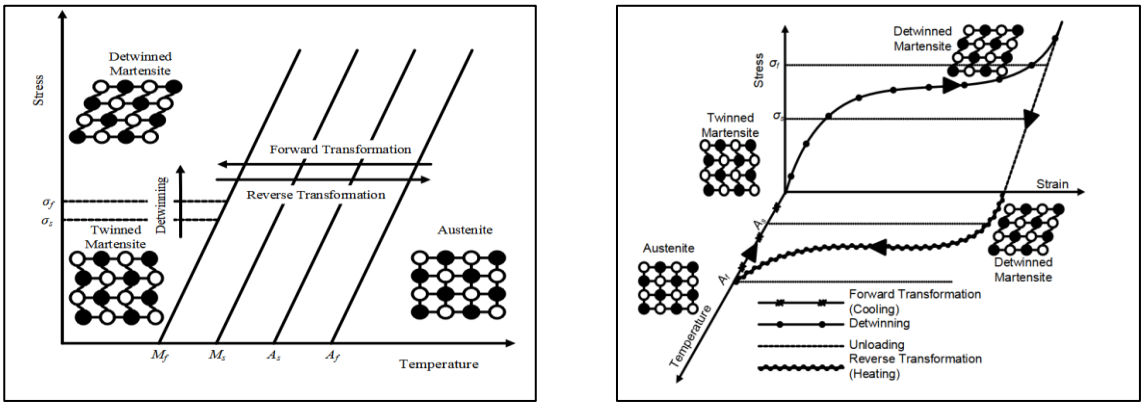

(a) (b)

Fig. 2. Temperature-induced phase transformation (a) Presence of applied load and (b) Data exhibiting the SME for a typical NiTi SMA [22]

If a force is exerted on the material while it is in the twinned martensitic phase, it can be possible to de-twin the structure of the martensite phase by reorienting a specific number of its variants as explained by Kumar and Lagoudas [22]. The de-twinning process results in a macroscopic shape change, where the deformed configuration is retained even after the load is released. Upon heating above A_f, the de-twinned martensite phase transforms to the austenite phase, causing the recovery of the deformation. This process is called the Shape Memory Effect (SME), which allows them to recover their original length and provide residual compressive stresses to the concrete after heating and cooling.

3. Finite Element Modelling

3.1 Concrete

In ABAQUS, there are three available methods: the smeared crack model, the brittle crack model, and the concrete damaged plasticity model as explained by Vilnay *et al.,* [23]. Generally, the smeared crack concrete model can be applied to model concrete in all types of structures and can be used for plain concrete, even though it is primary intended for the analysis of RC structures. However, it was suggested that this particular approach is suitable for situations where the concrete material is mostly subjected to constant or monotonic stress rather than cyclic or dynamic load. Additionally, it may not accurately model individual cracks or defects that occur in the concrete on a large scale. The brittle cracking model can define proper concrete behaviour in the post-cracking stage, but it assumes that concrete behaves elastically under compression. The principle of this method is that it is designed for applications in which the behaviour is dominated by tensile cracking and the compressive behaviour is always linear elastic [24]. This study adopted the concrete damaged plasticity (CDP) model by Hafezolghorani *et al.,* [25] to model the behaviour of concrete materials.

The significant advantage of the CDP model over the smeared crack model is the efficient convergence of calculations. The mechanical properties of the concrete are summarised in Table 1. An 8-node linear brick with reduced integration and an hourglass (C3D8R) is used as the element to model the concrete element.

Table 1
Concrete Properties [10]

Plasticity Parameters	
Dilation angle, (°)	31
Plastic potential eccentricity	0.1
Stress ratio, Fb0/fc0	1.16
Shape of the yielding surface, K	0.67
Viscosity parameter, μ	0.0001

3.2 Steel Reinforcements

In ABAQUS, the reinforcements can be modelled in two ways: either as a solid part or as a wire part. If the reinforcements are modelled using a solid part, it will be modelled as a cylinder, while for wire, a line is used to idealise a solid reinforcement in which its thickness and depth are considered small compared to its length. In this study, the reinforcements are modelled as a wire part. Table 2 tabulates the reinforcements' properties utilised in this study.

Table 2
Steel reinforcements' properties

Rebar diameter	Young Modulus, MPa	Poisson's ratio	Yield stress, MPa
10 mm	200000	0.3	561
12 mm	200000	0.3	566

To model the reinforcement as a wire element, a 2-node linear 3-D (T3D2) truss element was assigned to the reinforcement that provided only the axial stiffness. This approach allows for a simplified representation of the reinforcement behaviour, as the axial stiffness of the wire element can be easily calculated and incorporated into the overall stiffness matrix of the truss structure.

3.3 Iron-Based Shape Memory Alloy (Fe-SMA)

The Fe-SMA rebar material's behaviour is assumed to exhibit isotropic hardening plasticity. To implement the behaviour of activated Fe-SMA in the RC beam, only the failure segment of the curve is defined as the input as per Abouali *et al.,* [26], as presented in Figure 3.

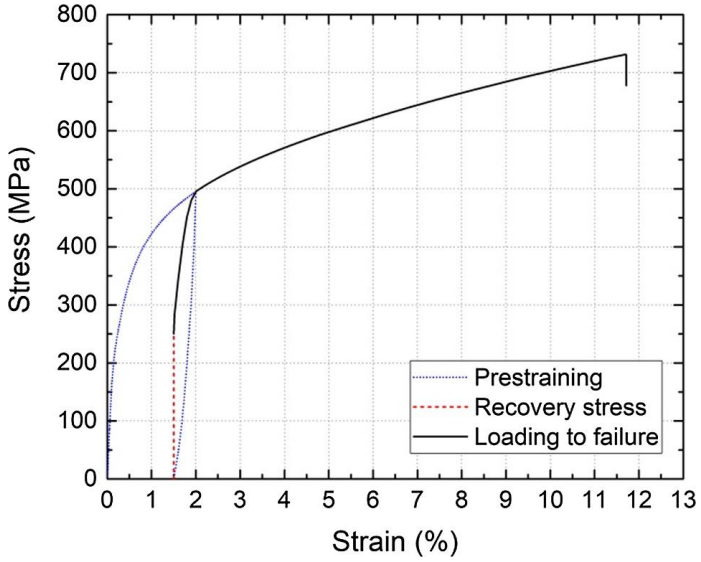

Fig. 3. Stress-strain curve of activated Fe-SMA [26]

The physical properties of Fe-SMA adopted in this study are taken from Zhang *et al.,* [21], as presented in Table 3. To model the prestressing of the Fe-SMA rebar, an initial stress equal to the recovery stress generated by Fe-SMA rebars is used.

Table 3
Physical properties of Fe-SMA [21]

Fe-SMA	
Density	7.2–7.5 g/cm^3
Young's modulus	170 GPa
Electrical resistivity	100–130 μΩ·cm
Specific Heat Capacity	540 J/kg·◦C
Thermal Conductivity	8.4 W/(m·◦C)
Thermal expansion Coefficient	16.5 (×10−6) ◦C^{-1}
Melting Point	1320–1350 ◦C
Strain recovery limit	2%
Poisson's ratio	0.359

3.4 Loadings and Boundary Condition

In order to investigate the performance of the beam, a four-point flexural test was conducted. This test involves applying loads to the beam at two points along its length while measuring the reaction forces and deflection of the beam. Figure 4 illustrates the four-point flexural test setup. The RC models were analysed using the displacement-controlled loading method. A downward vertical displacement was applied to the loading point. Both supports were assigned boundary conditions of pinned reactions. The reaction force at the supports was calculated to obtain the load-deflection curve. The reinforcement was embedded in the concrete by applying an 'embedded region' constraint. Similarly, to simplify the model, the Fe-SMA elements were also embedded in the concrete, as suggested by Abouali *et al.,* [26]. An initial stress equal to the recovery stress of the Fe-SMA bars was used to define the prestressing force. In this model, a 'Static, General' analysis was employed to study the behaviour of the system under various loads and boundary conditions.

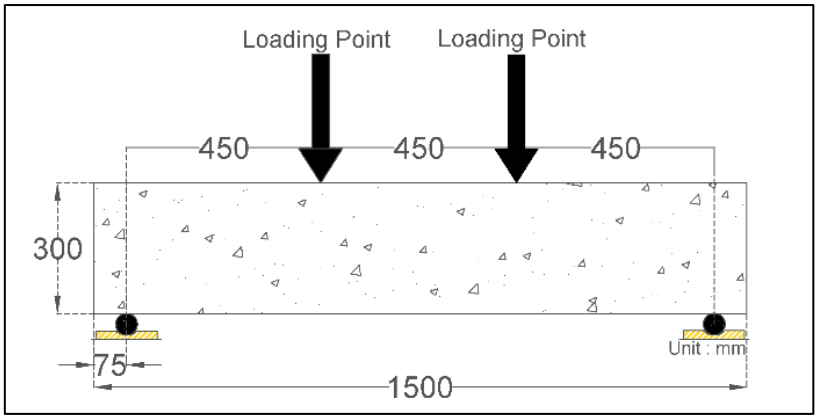

Fig. 4. Details of the four-point setup

4. Results

4.1 Validation of Finite Element Modelling

To ensure the accuracy and reliability of FE modelling for analysing RC strengthened with NSM Fe-SMA RC rebars, a validation was done with previous work done by Geetha and Selvakumar [27]. Two (2) RC beams with dimensions of 150 mm height, 300 mm width, and 1500 mm length were modelled: one strengthened with Fe-SMA bars at the tensile region (Fe Model-FeSMA) and another unstrengthen RC beam (FE Model-Control). A four-point load test is applied to the beam to measure its deflection and load carrying capacity. By conducting a thorough validation process, the performance of RC beams under FE modelling can be evaluated to ensure the optimisation task has been configured correctly.

4.1.1 Mesh convergence study

The mesh convergence test is important as it ensures the accuracy and reliability of numerical simulations by assessing the convergence of results with varying mesh sizes. Although a smaller mesh size is preferred for generating more accurate results, it also leads to increased computational time in FE modelling. Based on Geetha and Selvakumar [27] study, the convergence test is done for FE Model-Control specimens. A decrease in the load from 94.35 kN to 81.040 kN was seen when the mesh size was reduced from 200 mm to 40 mm, as presented in Table 4.

Table 4
Result of Mesh Convergence Study

Mesh Size, mm	Maximum Load, kN	Computational time, min
200	94.35	1
150	93.37	1
100	76.21	2
75	74.47	2
50	78.44	5
45	77.44	6
40	81.04	8
35	80.15	17
30	80.20	29
25	79.26	44
20	80.03	92

However, fluctuations in the load values occurred as the mesh size decreased further. From a mesh size of 40 mm and below, the load-capacity of the RC beam stabilised within the range of 79.26 kN to 81.04 kN, indicating convergence. Based on these results, a mesh of approximately 45 mm or smaller is recommended. Therefore, at a mesh size of 30 mm, the load value of 80.20 kN was within the stable range observed for smaller mesh sizes. Selecting a mesh size of 30 mm provides a reasonable compromise between accuracy and computational efficiency. By adopting this mesh size, computational time is reduced compared to using a smaller mesh size, such as 25 mm, while still obtaining reliable and convergent results.

4.1.2 Validation results

Table 5 tabulates the results of the ultimate load and deflection from the four-point bending tests conducted by Geetha and Selvakumar [27] and the numerical values obtained in this study. It is reported that the ultimate load for the control beam FE Model-Control obtained in their study was 80 kN and the maximum deflection was 15 mm. As compared to this study's Experimental-Control, the ultimate load obtained was slightly higher, at 80.20 kN, and the maximum deflection obtained was 14.3 mm. However, the results of the RC beam FE Model-FeSMA recorded a lower ultimate load of 119.37 kN compared to the similar beam of 118 kN, but the RC beam FE Model-Fe-SMA reported a lower deflection of 13.54 mm as compared to the RC beam Experimental-FeSMA of 14.7 mm. Based on the results, it is shown that the percentage of error for ultimate load is 1.15% and 8% for the mid-span deflection.

Table 5
FE validation model results

	Control			Fe-SMA		
	FE Model-Control	Experimental-Control	Percentage Error, %	FE Model-FeSMA	Experimental-FeSMA	Percentage Error, %
Ultimate Load, kN	80.00	80.20	0.25	118.00	119.37	1.15
Mid- span Deflection, mm	15.00	14.30	4.00	15.88	13.54	8.00

The numerical simulations were generally consistent with past paper experimental data, as presented in Figure 5, indicating that the FE models were capable of predicting the RC beam behaviour successfully under four-point bending. Variability in material properties and construction methods, as well as differences in loading conditions and testing setups, could contribute to slight differences in the results.

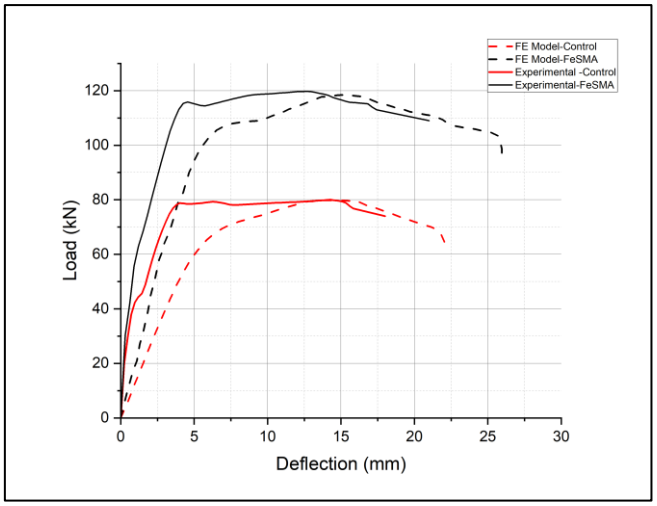

Fig. 5. Load-Deflection Curve of FE model results against the experimental results [27]

4.2 Beams Strengthened with NSM Fe-SMA Rebar

After the validation with the works done by Geetha and Selvakumar [27] was executed, a similar methodology was applied to model the control, 1-SMA, and 2-SMA RC beams. This study employed three (3) simply supported beams of 1.5 metres in length. The height and width of the beam were 300 mm and 200 mm, respectively. The first beam modelled was the control beam, which contained no additional rebar for the purpose of strengthening. The second model was the RC beam strengthened with one Fe-SMA bar (1-SMA), and the third model was the RC beam strengthened with two Fe-SMA bars (2-SMA), as presented in Figure 6. All the RC beams were modelled using the ABAQUS software. ABAQUS software is capable of modelling three-dimensional FE models of the beams proposed in the study [23,26].

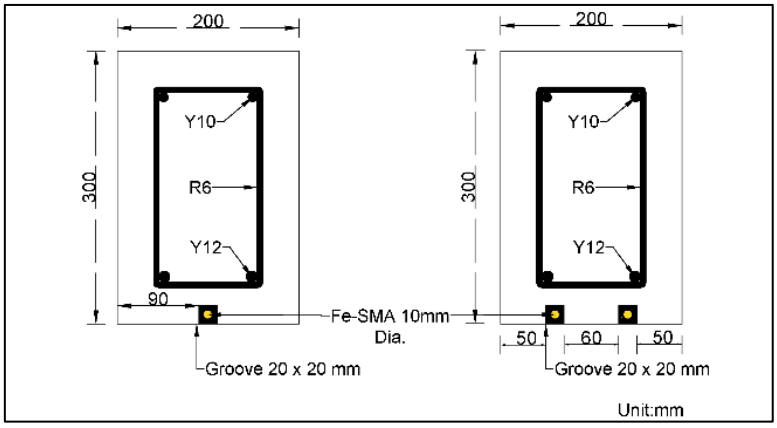

Fig. 6. Detail of RC Beam cross section proposed in this study

A total of three (3) FE models of the proposed RC beams strengthened with Fe-SMA were successfully modelled in this study to evaluate their flexural capabilities. To ensure that the FE models used in this study were valid, the results of the FE control beam and the RC beam strengthened with 1 Fe-SMA rebar (1-SMA) were compared to the experimental works from the study by Geetha and Selvakumar [27]. Figure 6 presents the comparison of load-deflection results obtained in this study to the experimental result. The numerical load-deflection curves from this study demonstrated good

agreement with the output from the study by Geetha and Selvakumar [27], which suggests that the FE model employed in this study accurately replicated the behaviour of the tested beam.

4.2.1 Load-Deflection NSM Fe-SMA

Figure 7 shows the results of the FE modelling of this study. The control beam showed a maximum load capacity of 152 kN with deflection at a mid-span of 5 mm, while the 1-SMA RC beam showed an increase of 17% in the load carrying capacity with a load of 178 kN as compared to the control beam. The 2-SMA RC beam demonstrated even greater improvement with a maximum load capacity of 224 kN, which is 25% more than the 1-SMA RC beam and 47% more than the control beam. These results indicated that strengthening RC beams using Fe-SMA bars can greatly improve the flexural strength of a RC member. Hence, it is important to note that Fe-SMA bars can be an effective solution for improving the performance of RC beams under flexural loading, especially for retrofitting purposes.

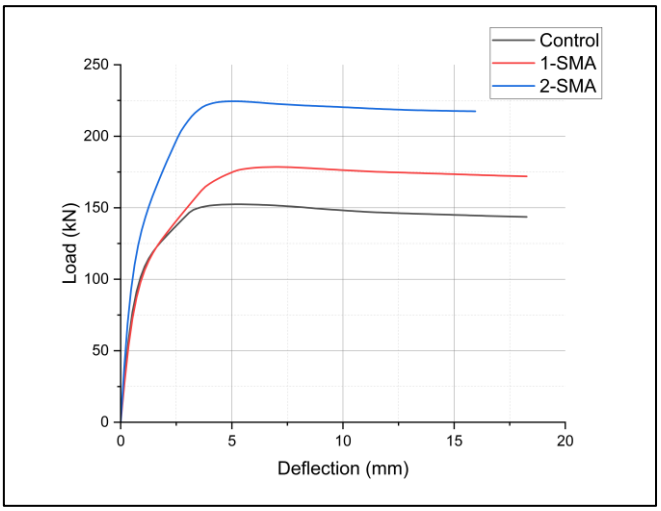

Fig. 7. Load-deflection curve of Fe NSM Fe-SMA

5. Conclusions

This study demonstrated the FE approach on the RC beams strengthened with Fe-SMA rebars, which could be applied in real applications for retrofitting purposes in RC structures using the NSM technique. In this study, the performance of RC beams strengthened using Fe-SMA rebar was explored numerically by developing three (3) different FE models in ABAQUS. The following conclusions are made based on the obtained results:

i. Based on the comparison between the finite element model Fe-SMA strengthened beam results and the literature values, it can be concluded that the model has an error of 1.15% in terms of ultimate load and a 14% error for deflection.
ii. The 2-SMA RC beam showed a maximum load capacity of 224 kN, which is 47% more than the control beam, indicating that Fe-SMA bars can greatly improve the flexural strength of RC beams.
iii. The application of Fe-SMA rebars can reduce the retrofitting cost effectively and improve the RC beam's flexural strength. This is due to the fact that in its actual application, this smart material does not require any prestressing tools and can be applied easily using the NSM technique, even in a small working space.

Acknowledgement

This study was funded by the Ministry of Higher Education Malaysia under Fundamental Research Grant Scheme (FRGS/1/2021/TK0/UITM/02/41). The authors would also like to thank Universiti Teknologi MARA, Cawangan Pulau Pinang for all the supports.

References

[1] Chang, Lo C., and T. A. Read. "Plastic deformation and diffusionless phase changes in metals—The gold-cadmium beta phase." *Jom* 3 (1951): 47-52. https://doi.org/10.1007/BF03398954

[2] Janke, L., Ch Czaderski, M. Motavalli, and J. Ruth. "Applications of shape memory alloys in civil engineering structures—Overview, limits and new ideas." *Materials and structures* 38 (2005): 578-592. https://doi.org/10.1007/BF02479550

[3] Qiang, Xuhong, Yapeng Wu, Yuhan Wang, and Xu Jiang. "Research Progress and Applications of Fe-Mn-Si-Based Shape Memory Alloys on Reinforcing Steel and Concrete Bridges." *Applied Sciences* 13, no. 6 (2023): 3404. https://doi.org/10.3390/app13063404

[4] Pirah, Jeffery Anak, Md Azree Othuman Mydin, Mohd Nasrun Mohd Nawi, and Roshartini Omar. "Innovative Application of Interwoven Fiberglass Mesh to Strengthen Lightweight Foamed Concrete." *Journal of Advanced Research in Applied Sciences and Engineering Technology* 28, no. 3 (2022): 165-176. https://doi.org/10.37934/araset.28.3.165176

[5] Cladera, Antoni, Benedikt Weber, Christian Leinenbach, Christoph Czaderski, Moslem Shahverdi, and Masoud Motavalli." Iron-based shape memory alloys for civil engineering structures: An overview." *Construction and building materials* 63 (2014): 281-293. https://doi.org/10.1016/j.conbuildmat.2014.04.032

[6] Debbarma, S. R., and S. Saha. "Review of Shape Memory Alloys applications in civil structures, and analysis for its potential as reinforcement in concrete flexural members." *International Journal of Civil & Structural Engineering* 2, no. 3 (2012): 924-942. https://doi.org/10.6088/ijcser.00202030020

[7] Hasnat, Abul, Safkat Tajwar Ahmed, and Hafiz Ahmed. "A review of utilizing shape memory alloy in structural safety." *AIUB Journal of Science and Engineering (AJSE)* 19, no. 3 (2020): 116-125. https://doi.org/10.53799/ajse.v19i3.111

[8] Dong, Zhiqiang, Ziqing Liu, Jianghao Ji, Hong Zhu, Gang Wu, and Changjun Sun. "Characterization of self-prestressing iron-based shape memory alloy bars for new structures." *Construction and Building Materials* 371 (2023): 130795. https://doi.org/10.1016/j.conbuildmat.2023.130795

[9] Ji, Jianghao, Zhiqiang Dong, Ziqing Liu, Yu Sun, Hong Zhu, Gang Wu, and Chee-Kiong Soh. "Feasibility of using Fe-SMA rebar as cracking resistance spiral stirrup in the anchorage zone of post-tensioned prestressed concrete." In *Structures*, vol. 48, pp. 823-838. Elsevier, 2023. https://doi.org/10.1016/j.istruc.2023.01.011

[10] Suhail, R., G. Amato, M. Shahria Alam, B. Broderick, M. Grimes, and D. McCrum. "Seismic retrofitting of nonseismically detailed exterior reinforced concrete beam-column joint by active confinement using shape memory alloy wires." *Journal of Structural Engineering* 149, no. 3 (2023): 04023003. https://doi.org/10.1061/JSENDH.STENG-11843

[11] Hamid, Nubailah Abd, Azmi Ibrahim, Azlan Adnan, and Muhammad Hussain Ismail. "Behaviour of smart reinforced concrete beam with super elastic shape memory alloy subjected to monotonic loading." In *AIP Conference Proceedings*, vol. 1958, no. 1. AIP Publishing, 2018. https://doi.org/10.1063/1.5034565

[12] Yurdakul, Özgür, Onur Tunaboyu, and Özgür Avşar. "Retrofit of non-seismically designed beam-column joints by post-tensioned superelastic shape memory alloy bars." *Bulletin of Earthquake Engineering* 16 (2018): 5279-5307. https://doi.org/10.1007/s10518-018-0323-y

[13] Soroushian, Parviz, Ken Ostowari, Ali Nossoni, and Habibur Chowdhury. "Repair and strengthening of concrete structures through application of corrective posttensioning forces with shape memory alloys." *Transportation Research Record* 1770, no. 1 (2001): 20-26. https://doi.org/10.3141/1770-03

[14] El-Hacha, Raafat, and Hothifa Rojob. "Fatigue performance of RC beams strengthened in flexure using NSM iron-based shape memory alloy bars." In *Proceedings of the Third Conference on Smart Monitoring, Assessment and Rehabilitation of Civil Structures, Antalya, Turkey*, pp. 7-9. 2015.

[15] El-Hacha, Raafat, and Hothifa Rojob. "Flexural strengthening of large-scale reinforced concrete beams using near-surface-mounted self-prestressed iron-based shape-memory alloy strips." *PCI J* 63, no. 6 (2018): 51-62. https://doi.org/10.15554/pcij63.6-03

[16] Hong, Ki-Nam, Yeong-Mo Yeon, Sang-Won Ji, and Sugyu Lee. "Flexural behavior of RC beams using Fe-based shape memory alloy rebars as tensile reinforcement." *Buildings* 12, no. 2 (2022): 190. https://doi.org/10.3390/buildings12020190

[17] Michels, Julien, Moslem Shahverdi, and Christoph Czaderski. "Flexural strengthening of structural concrete with iron-based shape memory alloy strips." *Structural Concrete* 19, no. 3 (2018): 876-891. https://doi.org/10.1002/suco.201700120
[18] Shahverdi, Moslem, Christoph Czaderski, Philipp Annen, and Masoud Motavalli. "Strengthening of RC beams by iron-based shape memory alloy bars embedded in a shotcrete layer." *Engineering Structures* 117 (2016): 263-273. https://doi.org/10.1016/j.engstruct.2016.03.023
[19] Shahverdi, Moslem, Christoph Czaderski, and Masoud Motavalli. "Strengthening of RC beams with iron-based shape memory alloy strips." *SMAR 2015, Antalya, Turkey, 7-9 September 2015* 8 (2015).
[20] Rojob, Hothifa, and Raafat El-Hacha. "Ductility behavior of RC beams strengthened in flexure with NSM Iron-based Shape Memory Alloy bars." In *Proceedings of the Third Conference on Smart Monitoring, Assessment and Rehabilitation of Civil Structures, Antalya, Turkey*, pp. 7-9. 2015.
[21] Zhang, Zhe-Xi, Jie Zhang, Honglei Wu, Yuezhen Ji, and Dheeraj D. Kumar. "Iron-based shape memory alloys in construction: research, applications and opportunities." *Materials* 15, no. 5 (2022): 1723. https://doi.org/10.3390/ma15051723
[22] Kumar, P. K., and D. C. Lagoudas. "Introduction to shape memory alloys." In *Shape memory alloys: modeling and engineering applications*, pp. 1-51. Boston, MA: Springer US, 2008. https://doi.org/10.1007/978-0-387-47685-8_1
[23] Dolatabadi, Neda, Moslem Shahverdi, Mehdi Ghassemieh, and Masoud Motavalli. "RC Structures strengthened by an iron-based shape memory alloy embedded in a shotcrete layer—Nonlinear finite element modeling." *Materials* 13, no. 23 (2020): 5504. https://doi.org/10.3390/ma13235504
[24] Vilnay, Margi, Leon Chernin, and Demetrios Cotsovos. "Advanced material modelling of concrete in Abaqus." In *9th International Concrete Conference: Environment, Efficiency and Economic Challenges for Concrete, At University of Dundee Cite this publication*. 2014.
[25] Hafezolghorani, Milad, Farzad Hejazi, Ramin Vaghei, Mohd Saleh Bin Jaafar, and Keyhan Karimzade. "Simplified damage plasticity model for concrete." *Structural engineering international* 27, no. 1 (2017): 68-78. https://doi.org/10.2749/101686616X1081
[26] Abouali, Sahar, Moslem Shahverdi, Mehdi Ghassemieh, and Masoud Motavalli. "Nonlinear simulation of reinforced concrete beams retrofitted by near-surface mounted iron-based shape memory alloys." *Engineering Structures* 187 (2019): 133-148. https://doi.org/10.1016/j.engstruct.2019.02.060
[27] Geetha, S., and M. Selvakumar. "Self prestressing concrete composite with shape memory alloy." *Materials Today: Proceedings* 46 (2021): 5145-5147. https://doi.org/10.1016/j.matpr.2020.10.677